

The PTI Carbon Star Angular Size Survey: Effective Temperatures and Non-Sphericity

Gerard T. van Belle¹, Claudia Paladini², Bernhard Aringer³, Josef Hron², David Ciardi⁴

¹Lowell Observatory, ²Universität Wien, ³INAF-OAPD, ⁴Caltech

Abstract: We report new interferometric angular diameter observations of 41 carbon stars observed with the *Palomar Testbed Interferometer* (PTI). Two of these stars are CH carbon stars and represent the first such measurements for this subtype. Of these, 39 have Yamashita (1972, 1975) spectral classes and are of sufficiently high quality that we may determine the dependence of effective temperature on spectral type. We find that there is a tendency for the effective temperature to increase with increasing temperature index by ~ 120 K per step, starting at $T_{\text{EFF}} \approx 2500$ K for C3,y. Overall, the median effective temperature for the carbon star sample is found to be 2800 ± 270 K, and the median linear radius is $360 \pm 100 R_{\odot}$. We also find agreement on average within 15 K with the T_{EFF} determinations of Bergeat (2001, 2002a,b), and a refinement of carbon star angular size prediction based on V & K magnitudes is presented that is good to an rms of 12%.

A subsample of our stars have sufficient $\{u,v\}$ coverage to permit non-spherical modeling of their photospheres, and a general tendency for detection of statistically significant departures from sphericity with increasing signal-to-noise of the interferometric data is seen. The implications of most --- and potentially all --- carbon stars being non-spherical is considered in the context of surface inhomogeneities and a rotation-mass loss connection. A possible correlation between the increasing mass loss rates of Claussen (1987) and increasing oblateness is observed.

Figure 1a (left): Stellar limb fits for the carbon stars in this study, including circular (red solid line) and elliptical (green dotted line). Outlier data point at $\{-0.9, -1.1\}$ mas for HD19881, $\{-0.9, -0.7\}$ mas for HD144578 not included in fit data; outliers at $\{-0.8, -1.3\}$ mas for HIP92194 also discarded.

Figure 1a (right): Stellar limb fits for the carbon stars in this study, including circular (red solid line) and elliptical (green dotted line).

Figure 2: A comparison of our effective temperatures versus those from Bergeat et al. (2002). The two hottest objects, HD30443 & HD59643, are members of the 'hot carbon' group of Bergeat et al. (2001), also noted as CH subtypes by Yamashita et al. (1972, 1975b). CH stars are thought to be a distinct group of high-velocity carbon stars (Yamashita et al. 1975a).

Figure 3: Difference in reduced χ^2 fit values for elliptical versus circular on-sky photosphere fits; blue points are carbon stars, red points are the giant check stars. There is a general tendency for $\Delta\chi^2$ to increase with increasing angular size, which correlates with increased angular size SNR. From this trend, we derive a general expectation that non-sphericity will be seen for all stars of sufficient angular size.

Figure 4: From Yamashita (1972, 1975), a comparison of effective temperature versus spectral types for the common sample of 40 stars:

$$T_{\text{EFF}} = (117 \pm 13)x + (2183 \pm 72)$$

where $|(\Delta T)_{\text{ABS}}| = 152$ K and $\chi^2_v = 5.2$. As noted Figure 2, the two hottest objects are atypical and are not included in this fit. The indicated anti-correlation of T_{EFF} with Yamashita spectral subtype is consistent with the expectation from Tsuji et al. (1981) and the initial indications found in Dyck et al. (1996).

Figure 5: Our values for oblateness $\alpha_{ab} = a/b - 1$ versus mass loss rates from Claussen et al. 1987, with a fit line described by:

$$\alpha_{ab} = (0.11 \pm 0.06) \times \log_{10}(dM/dt) + (0.82 \pm 0.41)$$

with $\chi^2_v = 0.49$.

Figure 6: An example spectral energy distribution fit performed for this investigation. Using the model atmosphere of Aringer et al. (2009), F_{BOL} was derived, using the limb-darkened model atmosphere with $T_{\text{EFF}} = 2800$ K, $\log g = -0.40$, $M = 2M_{\odot}$, fit to HD2342 photometry with $A_V = 0.75$ mag.

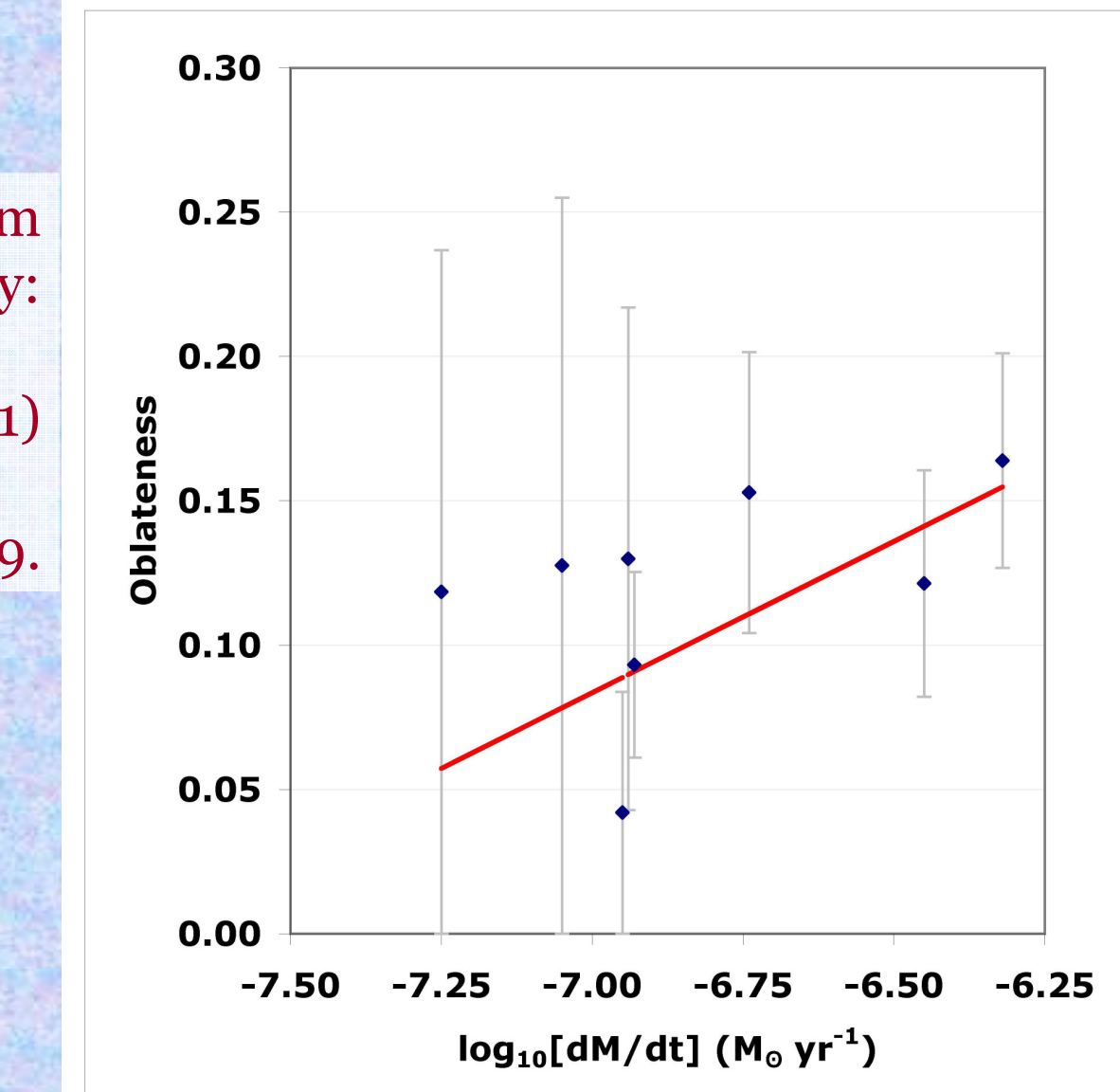
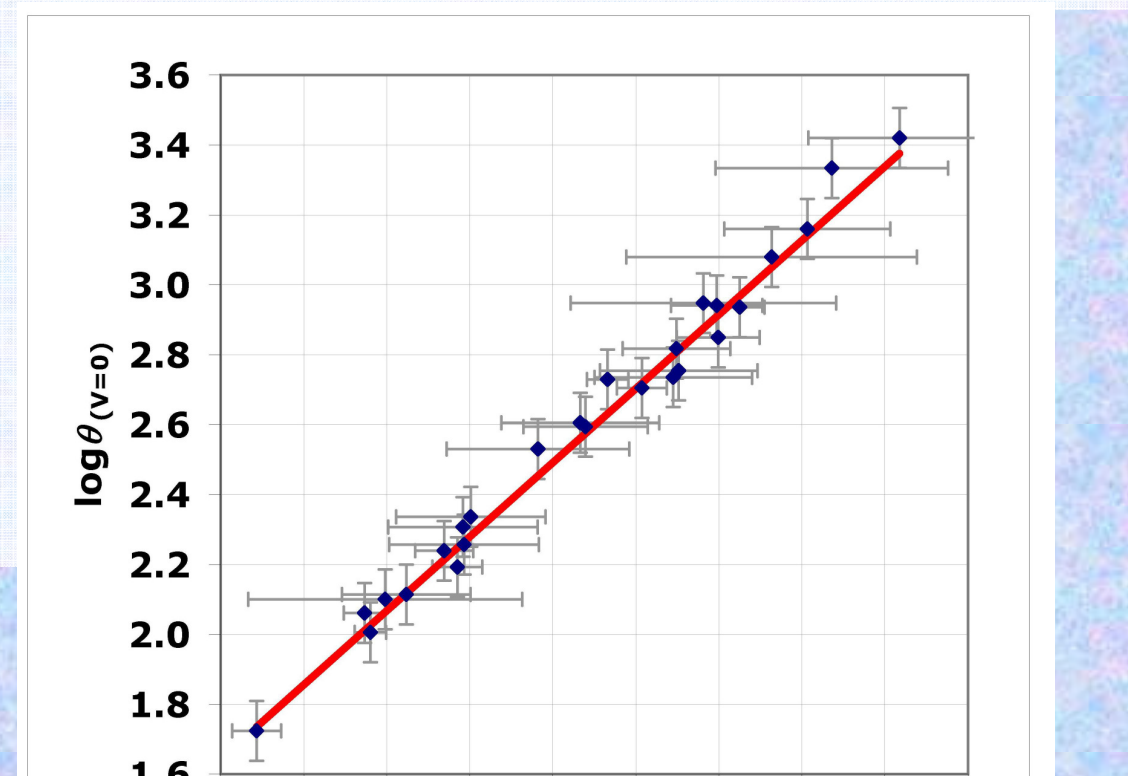


Figure 7: Reference angular sizes $\theta_{V=0}$ versus $V-K$ color, and associated fit:

$$\log_{10}\theta_{V=0} = (0.796 \pm 0.107) + (0.212 \pm 0.014) \times (V-K)$$

with a rms error of 12%; $V-K$ uncertainty in this plot is dominated by V variability. This represents a 2.2× improvement over the previous predictive fit in van Belle (1999).



Contact:
Gerard T. van Belle
Lowell NPOI Principal Investigator
gerard@lowell.edu

Parameters of ellipse fits to angular size data for those stars with semi-orthogonal NS and NW baseline data.

| Star ID | θ_{circ} (mas) | a (mas) | b (mas) | ϕ (deg) ^a | $\chi^2_{\nu, \text{ellipse}}$ | $\chi^2_{\nu, \text{circle}}$ | $\Delta\chi^2_{\nu}$ | θ_{equiv} (mas) | $\frac{\theta_{\text{equiv}}}{\theta_{\text{circ}}}$ | oblateness | $\alpha_{ab} = a/b - 1$ |
|-------------------------------------|---------------------------------|-------------------|-------------------|------------------------------|--------------------------------|-------------------------------|----------------------|----------------------------------|--|---------------------------|-------------------------|
| HD19881 | 2.371 ± 0.010 | 2.441 ± 0.085 | 2.165 ± 0.096 | -50 ± 8 | 1.1 | 1.6 | 0.4 | 2.298 | 0.969 | $0.128^{+0.093}_{-0.128}$ | |
| IRC+40067 | 3.297 ± 0.018 | 3.396 ± 0.079 | 3.005 ± 0.160 | -47 ± 6 | 0.8 | 1.7 | 0.8 | 3.194 | 0.969 | $0.130^{+0.087}_{-0.073}$ | |
| HD59643 | 1.499 ± 0.024 | 1.766 | 1.476 | 57 | 1.2 | 1.2 | 0.0 | 1.614 | 1.077 | 0.197 | |
| HD144578 | 1.642 ± 0.015 | 1.658 ± 0.036 | 1.612 ± 0.080 | -78 ± 1 | 2.2 | 2.1 | -0.1 | 1.635 | 0.995 | $0.029^{+0.096}_{-0.029}$ | |
| HIP92194 | 3.459 ± 0.004 | 3.917 ± 0.086 | 3.365 ± 0.016 | 28 ± 1 | 2.0 | 4.8 | 2.7 | 3.630 | 1.049 | $0.164^{+0.032}_{-0.037}$ | |
| HIP95024 | 3.808 ± 0.018 | 3.951 ± 0.048 | 3.588 ± 0.053 | -76 ± 12 | 0.1 | 14.1 | 14.1 | 3.765 | 0.989 | $0.101^{+0.040}_{-0.040}$ | |
| HIP95777 | 3.394 ± 0.010 | 3.634 ± 0.076 | 3.152 ± 0.062 | -54 ± 11 | 2.6 | 7.8 | 5.2 | 3.385 | 0.997 | $0.153^{+0.049}_{-0.049}$ | |
| HIP102764 | 2.391 ± 0.018 | 2.432 ± 0.048 | 2.174 ± 0.170 | -62 ± 12 | 1.2 | 1.5 | 0.3 | 2.300 | 0.962 | $0.118^{+0.065}_{-0.065}$ | |
| HIP105539 | 2.619 ± 0.005 | 2.776 ± 0.047 | 2.539 ± 0.022 | 42 ± 1 | 2.2 | 3.2 | 1.0 | 2.655 | 1.014 | $0.093^{+0.026}_{-0.032}$ | |
| HIP113713 | 2.450 ± 0.004 | 2.530 ± 0.030 | 2.429 ± 0.010 | 66 ± 11 | 3.8 | 4.0 | 0.2 | 2.479 | 1.012 | $0.042^{+0.042}_{-0.042}$ | |
| HD220870 | 1.901 ± 0.007 | 1.940 ± 0.020 | 1.839 ± 0.027 | -75 ± 18 | 0.9 | 1.3 | 0.4 | 1.889 | 0.993 | $0.055^{+0.049}_{-0.055}$ | |
| Check stars (NS, NW baselines only) | | | | | | | | | | | |
| HD113226 | 3.062 ± 0.009 | 3.073 ± 0.096 | 3.001 ± 0.073 | -7 ± 42 | 2.1 | 1.9 | -0.2 | 3.037 | 0.992 | $0.024^{+0.033}_{-0.024}$ | |
| HD216131 | 2.366 ± 0.011 | 2.388 ± 0.159 | 2.344 ± 0.056 | 29 | 0.3 | 0.3 | 0.0 | 2.366 | 1.000 | $0.019^{+0.071}_{-0.019}$ | |
| Check stars (all baselines) | | | | | | | | | | | |
| HD113226 | 3.066 ± 0.008 | 3.088 ± 0.030 | 3.018 ± 0.054 | 10 ± 9 | 1.8 | 1.8 | 0.0 | 3.053 | 0.996 | $0.023^{+0.028}_{-0.023}$ | |
| HD216131 | 2.369 ± 0.010 | 2.395 ± 0.047 | 2.333 ± 0.047 | 27 | 0.3 | 0.5 | 0.1 | 2.364 | 0.998 | $0.027^{+0.036}_{-0.027}$ | |

^a No error given for $\{a, b, \phi\}$ or oblateness $\alpha_{ab} = a/b - 1$ indicates that the error term was not constrained by examination of the $\Delta\chi^2_{\nu, \text{ellipse}}$ surface.

Table 1: Circular and ellipsoidal fits to PTI data for carbon stars with NS and NW baseline data.